On-chip investigation of phase noise in monolithically integrated gain-switched lasers

Justin K. Alexander, Padraic E. Morrissey, Ludovic Caro, Mohamad Dernaika, Niall P. Kelly, and Frank H. Peters.

June 8, 2018

Abstract

Phase noise in gain-switched lasers is investigated theoretically using the semiconductor laser rate equations and compared to experimental results from monolithically integrated devices. The phase noise of a gain-switched laser is modelled both with and without injection-locking using the rate equations for a single-mode laser. Phase noise is found to increase with gain-switching, and decrease when injection-locked to a master laser. This trend is then observed experimentally on-chip with monolithically integrated devices without the use of an isolator.

1 Introduction

Coherent wavelength division multiplexing (CoWDM) aims to increase the spectral efficiency of optical communications by specifying coherence between carriers [1]. A set of coherent channels is referred to as a super-channel, and an optical comb source is a key component in creating the super-channel [2]. Gain-switching is a comb generation technique where a laser is directly modulated by a high power RF signal. The comb line spacing can be adjusted by changing the frequency of the RF signal. The straight forward implementation and flexibility makes gain-switching appear to be a prime candidate for the generation of optical combs for CoWDM. However, an inherent limitation in the technique is the increase in phase noise due to the modulation of the laser carriers. The oscillation of the carrier number leads to an oscillation of the refractive index of the cavity, leading to a chirp in the output frequency of the laser. The chirp can be seen as an increase in the laser linewidth. A recent study has shown that gain-switching a laser beyond the devices bandwidth can minimise the increase in linewidth [3], although the problem still remains of designing a laser with both a low linewidth and large bandwidth.

Injection-locking has been demonstrated to decrease the linewidth of a directly modulated laser [4], as well as increasing the laser bandwidth [5]. A low linewidth master laser injection-locks the directly modulated slave laser, with the resulting linewidth similar to that of the master. A low-linewidth comb source has recently been demonstrated based on injection-locked gain-switched lasers [6].

In this letter, a theoretical analysis of the phase noise in gain-switched lasers is performed using the semiconductor laser rate equations, both with and without injection-locking. The trends in phase noise from the modelled equations are then compared to monolithically integrated devices which were designed, fabricated, and characterised. Injection-locking is performed on-chip without the use of an optical isolator.

2 Rate equations

2.1 Without injection-locking

The rate equations for a single mode laser are given by [3],

$$\frac{dN}{dt} = \frac{I(t)}{eV} - R(N) - \Gamma a(N - N_{tr})S + F_N(t) \tag{1}$$

$$\frac{dS}{dt} = \left(\Gamma a(N - N_{tr}) - \frac{1}{\tau_p}\right) S + \beta BN^2 + F_S(t) \tag{2}$$

$$\frac{d\phi}{dt} = \frac{1}{2}\Gamma\alpha_H a(N - N_{tr}) + F_\theta(t) \tag{3}$$

where N is carrier density, S is photon density, ϕ is phase, $I(t)$ is the input current, $R(N)$ is the rate of carrier recombination including the non-radiative, bimoleculor, and Auger recombination.

$$R(N) = AN + BN^2 + CN^3 \tag{4}$$

$F_N(t)$, $F_S(t)$, and $F_\theta(t)$ are Langevin noise sources based on Gaussian random variables and are outlined elsewhere [7]. Additional terms, as well as terms used later, are defined in Table.1.

Table 1: Parameter definitions and values

Parameter	Definition	Value
e	Electron charge	$1.602e^{-19}\ C$
V	Volume of active region	$1.125e^{-17}\ m^3$
L	Length of device	$500e^{-6}\ m$
Γ	Confinement factor	0.3
a	Differential gain	$5e^{-13}\ m^3 s^{-1}$
N_{tr}	Carrier density at transparency	$1e^{-24}\ m^{-3}$
τ_p	Photon lifetime	$4.8e^{-12}\ s$
β	Fraction of spontaneous emission into lasing mode (slave/master)	$1e^{-4}/1e^{-9}$
a_H	Linewidth enhancement factor	4
A	Nonradiative recombination rate	$1e^{9}\ s^{-1}$
B	Bimoleculor recombination coefficient	$1e^{-16}\ m^{-3}s^{-1}$
C	Auger recombination coefficient	$1e^{-41}\ m^{-6}s^{-1}$
ν_g	Group velocity	$8.5e^{7}\ m\ s^{-1}$

The β parameter is artificially used to adjust the linewidth of the simulated lasers in the model.

2.2 With injection-locking

The rate equations for an injection-locked single mode laser are given by,

$$\frac{dN}{dt} = \frac{I(t)}{eV} - R(N) - \Gamma a(N - N_{tr})S + F_N(t) \tag{5}$$

$$\frac{dS}{dt} = \left(\Gamma a(N - N_{tr}) - \frac{1}{\tau_p}\right) S + \beta BN^2 + k_C\sqrt{S(t)S_{ml}(t)cos(\phi_{ml} - \phi)} + F_S(t) \tag{6}$$

$$\frac{d\phi}{dt} = \frac{1}{2}\Gamma\alpha_H a(N - N_{tr}) + k_C\sqrt{\frac{S_{ml}(t)}{S(t)}}sin(\phi_{ml} - \phi) - 2\pi\Delta f + F_\theta(t) \tag{7}$$

Where $k_C = \nu_g/2L$ is the coupling rate, $S_{ml}(t)$ is the master laser photon density, ϕ_{ml} is the master laser phase, and Δf is the frequency detuning between the master and the slave lasers (set to 0 in this case). All other terms are as before.

2.3 Phase noise

The instantaneous frequency variation can be calculated as;

$$\Delta v = \frac{1}{2\pi}\frac{d\phi}{dt} \tag{8}$$

The frequency noise (FN) spectrum can then be calculated from the Fourier transform of 8,

$$FN = \frac{1}{T}|\int_0^T \Delta v\tau e^{-j\omega\tau} d\tau|^2 \tag{9}$$

At low frequencies carrier/index fluctuations contribute to a higher white noise level [8], thus the average value of the low frequency ($< 1\,\text{GHz}$) FN spectrum times π is equivalent to the laser linewidth [9].

3 Theoretical analysis

The non-injection-locked rate equations (1, 2, 3) were solved in Matlab using the built in ordinary differential equation solver ODE45, which uses the 4^{th} order Runga-Kutta method to solve the equations numerically. The current was set to a constant 50 mA. The FN spectrum is plotted for two lasers of length 500 µm with β parameters of 10^{-4} and 10^{-8} in Figure 1. 10 averages were taken to smooth the trace. The increase in FN is clearly seen as the value of β is increased.

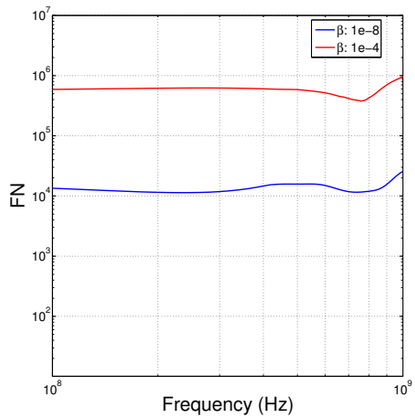

Figure 1: FN spectrum for two 500 µm lasers with β parameters of 10^{-4} and 10^{-8}.

For the injection-locked rate equations (5, 6, 7) the lower frequency noise laser was used as the master, with the higher frequency noise laser the slave. The equations were solved for the case of the slave gain-switched at 3 GHz. with no injection, and for the case of the slave gain switched with injection from the master. Gain-switching was applied to the slave laser by adding a cosine term to the current, $I = I + I_m cos(2\pi f)$, where $I = I_m = 50\,\text{mA}$ and $f = 3\,\text{GHz}$. While gain-switched, the laser is fundamentally a single mode laser, therefore the rate equations are still applicable. The frequency noise for these configurations is plotted in Figure 2 along with the free running master and slave frequency noise.

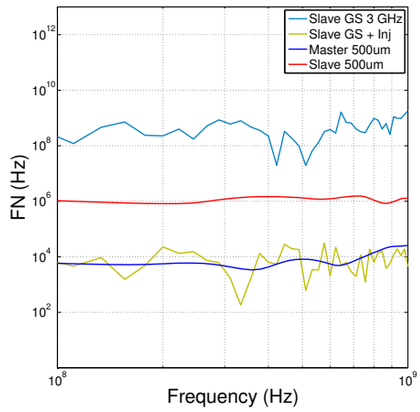

Figure 2: FN spectrum showing increase in frequency noise during gain-switching, and decrease with injection-locking. Free running master and slave included.

The frequency noise of the gain-switched slave is shown to decrease to that of the master while injection-locked.

4 Design and fabrication of devices

Two devices were fabricated for the purpose of investigating the frequency noise of gain-switched lasers. The devices were fabricated using commercially available lasing material consisting of 5 compressively strained AlGaInAs quantum wells on an n-doped (100) InP substrate, with a total active region thickness of 0.41 µm. The upper p-doped cladding consists of a 0.2 µm InGaAs cap layer, followed by 0.05 µm of InGaAsP, lattice matched to 1.62 µm of InP. The fabrication process is similar to the process described in [10]. Standard UV lithographic techniques were used to define the ridge and slot features, with a ridge width of 2.5 µm, ridge height 1.79 µm (shallow etch), deep etch depth 3 µm, and a slot width of 1 µm, with the ridge etch stopping above the quantum wells. All features were etched with an Inductively Coupled Plasma (ICP) etcher with etch chemistry $Cl_2/CH_4/H_2$ (Ratio 10:8:4)

Device 1 is a 2-section slotted Fabry-Perót (SFP) laser [11] with a total length of 1350 µm. The slotted section features 7 equally spaced slots with a slot spacing of 114 µm, connected to a straight 550 µm long gain section. A deep etch (3 µm deep) is used to define both the etched facets and a top level N-contact. A shallow etch of 1.79 µm through the P-doped region, stopping above the quantum wells, is used to define the ridge waveguides and SFP slots. Gold contact pads were deposited while simultaneously depositing gold over the etched facet of the slotted section in order to increase reflectivity [12]. The gain section features a cleaved facet. A schematic of the device can be seen in Figure 3a with the metal etched facet (MEF) labelled.

Device 2 is a SFP laser with a total length of 1890 µm, coupled to a 400 µm long FP laser via an etched facet. The SFP features the same slotted section as in device 1, with a 690 µm gain section. Light is coupled out of the device through the cleaved facet of the FP laser. The FP laser (slave laser) will be gain-switched and injection-locked to the on-chip SFP laser (master laser). Any change in frequency noise due to gain-switching will be measured by the linewidth of the output.

5 Experimental results and discussion

The devices were mounted on a thermally controlled brass chuck maintained at 23 °C. Light was coupled from the cleaved facet of the device with a lensed optical fibre. Optical spectra were recorded using an optical spectrum analyser (OSA) with a wavelength resolution of 0.015 nm. DC probes were used to bias each section with a GS (ground-signal)

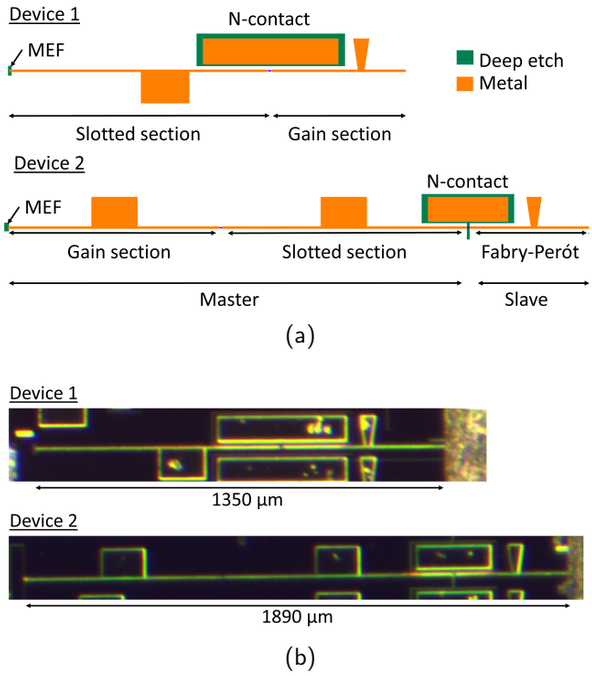

Figure 3: (a) Schematic of fabricated devices with sections labelled. (b) Microscope image of fabricated devices.

probe used to bias and modulate the FP laser. A bias tee was used to provide simultaneous DC & RF signals to the gain section of the laser.

5.1 Device 1: No injection locking

The gain and slotted sections were biased at 35 mA each and an optical spectrum was recorded. The spectrum can be seen in Figure 4. The gain and slotted sections were then biased at 72 mA and 34 mA respectively, and a 6 GHz 21 dBm RF signal was applied to the gain section. The optical comb produced can be seen in Figure 4.

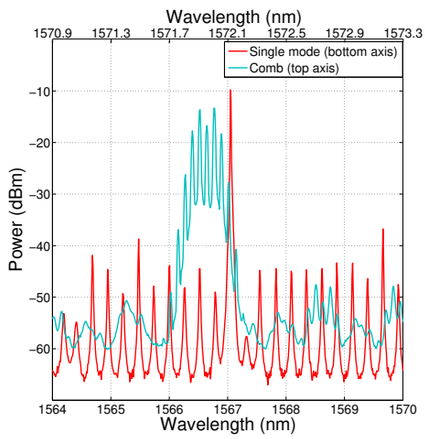

Figure 4: Single mode and 6 GHz optical comb spectra for device 1

.

The linewidth of the device was measured both before and after gain-switching, using the delayed self-heterodyne (DSH) method [6]. For an optical comb, the DSH gives the linewidth of the comb set, thus providing a weighted average linewidth of all the comb lines. An electrical spectrum analyser (ESA) was used to record the measurement. With 50 km of optical fibre, the lowest measurable linewidth was <2 kHz (excluding ESA restrictions). The resolution bandwidth of the ESA was set to 100 kHz, with a sweep time of 60 ms. The full-width half-maximum (FWHM) of the DSH measurement before gain-switching was 400 kHz, increasing to 2 MHz for the gain-switched laser. The measurements can be seen in Figure 5.

The linewidth of the laser is calculated from half the FWHM of the DSH measurement, giving linewidths of 200 kHz and 1 MHz for the single mode output and comb line set respectively. A 5 times increase in frequency noise is observed after the laser is gain-switched.

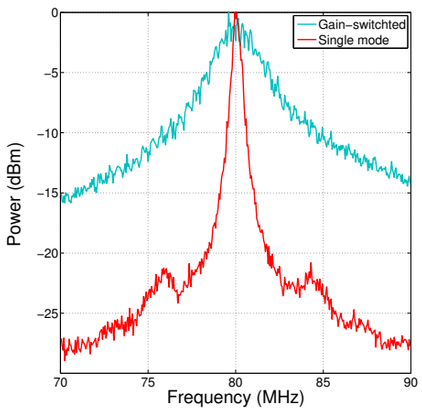

Figure 5: Overlapped linewidth measurement for device 1 before and after gain-switching.

5.2 Device 2: With injection locking

The gain and slotted sections were biased at 37 mA and 40 mA respectively, with the FP section biased at 40 mA. An optical spectrum was recorded. The spectrum can be seen in Figure 6. The gain and slotted sections were then biased at 35 mA and 51 mA respectively, with the FP biased at 57 mA. A 5 GHz 22 dBm RF signal was applied to the FP section. The optical comb produced can be seen in Figure 6.

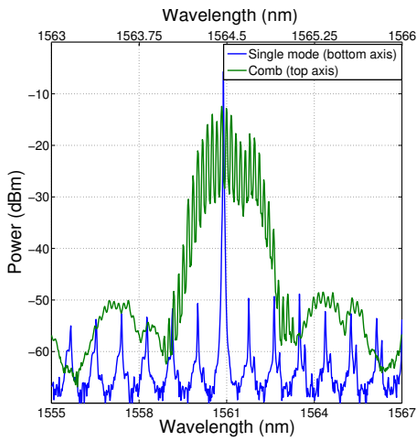

Figure 6: Single mode and 5 GHz optical comb spectra for device 2

The linewidth of the device was measured both before and after gain-switching, as with device 1. The FWHM of the DSH measurement before gain-switching was 700 kHz. After gain-switching the DSH measurement was also approximately 700 kHz. The measurements can be seen in Figure 7. This gives a linewidth of approximately 350 kHz with no major increase in frequency noise due to gain-switching. The linewidth of the FP laser with the master laser off could not be measured due to weak optical power output.

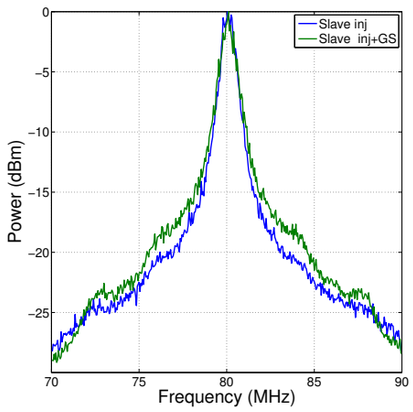

Figure 7: Overlapped linewidth measurement for device 2 before and after gain-switching.

Device 2 has a higher linewidth than device 1 for the non gain-switched case due to the increased loss in the cavity of device 2 from the deep etch slot. Higher loss in a cavity leads to a higher linewidth. Due to the impedance mismatch between the 50 Ohm signal generator and the laser as evaluated from S_{11} measurements using a vector network analyser (VNA), we estimate that 18% of the RF power was absorbed by device 1, and 21% was absorbed by device 2.

6 Conclusion

The frequency noise of a single mode laser tends to increases when gain-switched, while there is no observable increase in frequency noise for an injection-locked gain-switched laser. This trend has been demonstrated theoretically and experimentally as shown in Figures 2, 5 and 7. As device 1 is a two section device and only one section is gain-switched, the magnitude increase in phase noise is not as high as predicted by simulation. The refractive index of the mirror section is not oscillating, mitigating the overall phase noise increase. The device used standard UV lithographic techniques to minimize cost and complexity making this device a prime candidate for a CoWDM communications system. This work was supported by the Science Foundation Ireland under grants 12/RC/2276 (IPIC), SFI10/CE/I1853 (CTVR) and SFI/13/IA/1960.

References

[1] A. Ellis and F. Gunning, "Spectral density enhancement using coherent WDM," *IEEE Photonics Technology Letters*, vol. 17, no. 2, pp. 504–506, 2005.

[2] R. Nagarajan, M. Kato, D. Lambert, P. Evans, S. Corzine, V. Lal, J. Rahn, A. Nilsson, M. Fisher, M. Kuntz, J. Pleumeekers, A. Dentai, H.-S. Tsai, D. Krause, H. Sun, K.-T. Wu, M. Ziari, T. Butrie, M. Reffle, M. Mitchell, F. Kish, and D. Welch, "Terabit/s class InP photonic integrated circuits," *Semiconductor Science and Technology*, vol. 27, no. 9, p. 094003, 2012.

[3] P. M. Anandarajah, S. Member, R. Zhou, L. P. Barry, and S. Member, "Enhanced Optical Comb Generation by Gain-Switching a Single-Mode Semiconductor Laser Close to Its Relaxation Oscillation Frequency," vol. 21, no. 6, 2015.

[4] S. Mohidiek, H. Burkhard, and H. Walter, "Chirp reduction of directly modulated semiconductor lasers at 10 Gb/s by strong CW light injection," *Journal of Lightwave Technology*, vol. 12, no. 3, pp. 418–424, 1994.

[5] J. K. Alexander, P. E. Morrissey, H. Yang, M. Yang, and F. H. Peters, "Resonance Enhancement of a Monolithically Integrated Common Cavity Device," in *European Conference on Integrated Optics (ECIO)*, 2016.

[6] J. K. Alexander, P. E. Morrissey, H. Yang, M. Yang, P. J. Marraccini, B. Corbett, and F. H. Peters, "Monolithically integrated low linewidth comb source using gain switched slotted Fabry-Perot lasers," *Optics Express*, vol. 24, no. 8, p. 7960, 2016.

[7] I. Fatadin, D. Ives, and M. Wicks, "Numerical simulation of intensity and phase noise from extracted parameters for CW DFB lasers," *IEEE Journal of Quantum Electronics*, vol. 42, no. 9, pp. 934–941, 2006.

[8] C. H. Henry, "Theory of the Linewidth of Semiconductor Lasers," *IEEE Journal of Quantum Electronics*, vol. 18, no. 2, pp. 259–264, 1982.

[9] K. Kikuchi, "Characterization of semiconductor-laser phase noise and estimation of bit-error rate performance with low-speed offline digital coherent receivers," *Optics Express*, vol. 20, no. 5, p. 5291, 2012.

[10] P. E. Morrissey, N. Kelly, M. Dernaika, L. Caro, H. Yang, and F. H. Peters, "Coupled Cavity Single-Mode Laser Based on Regrowth-Free Integrated MMI Reflectors," *IEEE Photonics Technology Letters*, vol. 28, no. 12, pp. 1313–1316, 2016.

[11] D. Byrne, Q. Lu, W. H. Guo, J. F. Donegan, B. Corbett, B. Roycroft, P. Lambkin, J. P. Engelstaedter, and F. Peters, "A facetless laser suitable for monolithic integration," *2008 Conference on Quantum Electronics and Laser Science Conference on Lasers and Electro-Optics, CLEO/QELS*, pp. 2008–2010, 2008.

[12] C. Seibert and D. Hall, "High-index-contrast ridge waveguide laser with thermally oxidised etched facet and metal reflector," *Electronics Letters*, vol. 46, no. 15, p. 1077, 2010.